Evaluation of Aerodynamic Coefficients of Supercritical Airfoil NASA sc(2) 0712: A Comparative Study of 2D and 3D Flow Models with Experimental Validations

Teodora Šukunda
Vlatacom Institute
and
University of Belgrade
Faculty of Mechanical Engineering,
Belgrade, Serbia

Jelena Svorcan
University of Belgrade
Faculty of Mechanical Engineering,
Belgrade, Serbia

Toni Ivanov
University of Belgrade
Faculty of Mechanical Engineering,
Belgrade, Serbia

This study presents a comparative numerical analysis of 2D and 3D compressible, turbulent flows around the supercritical airfoil NASA sc(2) 0712 at Mach number M = 0.5 using the finite volume method implemented in ANSYS Fluent, focusing on the estimation of drag coefficients in relation to existing experimental data. In addition, different types of computational grids and turbulence models are tested. The investigation aims to highlight the discrepancies observed between the two modeling approaches and their implications for aerodynamic performance predictions. Through rigorous numerical simulations and validation against experimental results, we demonstrate that 2D models often yield overestimated drag values due to simplified flow assumptions. In contrast, 3D simulations provide a more accurate representation of fluid behavior, resulting in closer alignment with experimental findings. By performing spatial computations of turbulent flow around a supercritical airfoil, it is possible to reduce the relative error of drag coefficients by less than 10%.

Keywords: *Supercritical airfoil, Drag coefficient, CFD, Poly mesh, Mosaic elements, 3D versus 2D*

1. INTRODUCTION

Aerodynamic design and analysis involve significant challenges for engineers because of the many unresolved flow phenomena, along with the limitations and incomplete accuracy of numerical models, as well as the high cost and time–consuming nature of experiments. There is a desire to expand the operational range of the models that are being considered significantly. Accurate simulation and prediction of airflow around objects is crucial for their design, analysis, and optimization.

Traditional methods, such as analytical calculations based on empirical and theoretical models used in the initial design, can be time-consuming, and the results often have limitations characterized by the simpli–fication and idealization of conditions. Additi–onally, modeling turbulence and viscosity effects in analytical calculations are challenging, which can lead to an over or – underestimation of the actual drag. Furthermore, issues arise when modeling complex geometries, making it difficult to predict aerodynamic characte–ristics accurately. Some flight scenarios cannot be adequately captured through these techniques. This issue is particularly pronounced in the transonic flow regime.

Received: October 2024, Accepted: December 2024
Correspondence to: Teodora Šukunda
Vlatacom Institute, Milutina Milankovica 5, 11070 Belgrade, Serbia
E-mail: teodora.sukunda@vlatacom.com
doi: 10.5937/fme2501105S
© Faculty of Mechanical Engineering, Belgrade. All rights reserved

However, with the evolution of computational techniques, particularly finite volume method (FVM), and commercial software packages like ANSYS Fluent.

Using computational fluid dynamics (CFD) has significantly increased among engineers. Despite this, experimental testing cannot be entirely overlooked. Numerical analysis still needs to exhibit accuracy in calculating the boundary layer at the end of the shock wave, at higher angles of attack, and in cases of highly complex geometric shapes, particularly in the transonic regime. Therefore, it is essential to verify numerical calculations against existing experimental data. This verification process allows us to accurately validate the employed numerical models in areas where data is lacking. Paper [1] highlights the importance of comparing numerical calculations with wind tunnel experimental data. Comparing results enables the improvement of aerodynamic calculation methods, lea–ding to more accurate and reliable results, as described in detail in the paper. Also, in [2], the importance of comparing results is accentuated. In this study, numerical calculations were used to optimize the aerodynamic characteristics of the RAE 2822 transonic airfoil. Paper [3] describes how the supercritical–tran–sonic airfoil RAE 2822 was investigated numerically, and the obtained results were compared with expe–rimental data. The Spalart Allmaras turbulence model was applied and then compared using the k – w SST turbulence model. Similarly, in [4], excellent agreement was shown in predicting the transition from laminar to turbulent flow between numerical and experimental results. The numerical calculation was performed for the

supercritical airfoil NASA SR 0410 with the Spalart Allmaras turbulence model. In [5], the feasibility of CFD calculations in the context of preliminary analysis, with comparison with various other computational methods and software tools, was presented.

Wind tunnel testing can introduce additional uncertainties and errors, so performing a computational validation of the results is essential. Additionally, continuously comparing the wind tunnel results with computational methods is a key measure to ensure the accuracy and reliability of the data [6-8].

This study aims to examine flow around a super–critical airfoil specially designed for higher velocities and Mach numbers.

An airfoil is an aerodynamic shape that defines the form of a wing or other surfaces like stabilizers/tails or blades, depending on its application. Its primary pur–pose is to generate lift while minimizing drag, thereby providing optimal flight performance. The shape of an airfoil varies based on its intended operating range (from subsonic to supersonic), and this research focuses on the investigation of supercritical airfoils. Supercri–tical airfoils play a key role in design and optimization, and their development has been actively pursued for over a century. There are many families and a large variety of different airfoils.

Supercritical airfoils are specially designed aero–dynamic shapes optimized for high subsonic flight regimes [9]. Traditional airfoils have a curved upper surface, which allows for greater lift at subsonic speeds but also leads to an increase in drag at higher subsonic and transonic speeds.

On the other hand, supercritical airfoils feature a flat upper surface, which helps delay the shock wave towards the rear of the airfoil and sig–nificantly reduces wave drag at transonic flow condi–tions, which is crucial in the transonic flow regime.

In the following sections, a CFD analysis is perfor–med for the NASA SC (2) – 0712 airfoil. The results obtained from the numerical calculations are compared with available experimental data from NASA [10], highlighting the correlations presented below.

The information regarding the aerodynamic charac–teristics of this airfoil is quite limited. There are few studies that focus on the numerical analysis of the NASA sc (2) 0712 airfoil [11-13]. The investigation conducted in this study aims to provide a better understanding of the features of this revolutionary family of airfoils.

2. EXPERIMENTAL DATA

The experimental data used here was obtained in the two-dimensional test section of the Langley 0.3 Meter Transonic Cryogenic Tunnel [10]. In their investigation, the authors performed experimental testing of the NASA SC(3)-0712(B) airfoil with Mach numbers ranging from 0.5 to 0.8 and Reynolds numbers from 4.4 to 40 million. The angle of attack in the mentioned wind tunnel was adjusted automatically using computer control.

The NASA SC(3)-0712(B) airfoil designation is such that the number 3 refers to the development series, 0.7 represents the optimal lift coefficient, and 12 is the maximum relative thickness of the airfoil as a percentage.

The normal force coefficient in this investigation was obtained by numerical integration of the local pressures measured on 20 pressure orifices distributed equally along the airfoil surface. The local pressure coefficient, multiplied by a weighting factor, yields the value of Cn.

Although widely used, the applied measurement technique provides discrete results and is unable to capture the effects of viscosity.

The drag coefficient of the airfoil was obtained based on total pressure measurements using the Wake Survey Rake method (first employed by Johnson [14]), which measures the total pressure in tubes positioned directly behind the model. The drag coefficient is determined by reducing the measured pressure to dimensionless quantities and applying relevant for–mulas. This method also serves as a verification of the two-dimensionality of the flow around the model, as illustrated in Figure 1, but is also not completely accurate since it depends on the downstream location of the rake and the number of measuring points.

This testing is described in detail in the reference [15].

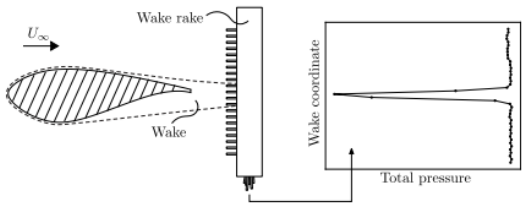

Figure 1. Scheme of Wake Rake method [15]

3. NUMERICAL ANALYSIS

An approach to solving the problem has been defined and presented in this study to ensure a credible examination of the flow around the airfoil. The analyses are divided into 2D and 3D computations. The primary objective of the investigation is to study the reliability of the 2D computations in the context of testing supercritical airfoils.

The 2D numerical computations in this study are based on a pressure–based model, combined with several different Reynolds – Averaged Navier Stokes (RANS) turbulence models [16]: k – w SST, k – ε standard, k – ε realizable, and the Spalart-Allmaras model. The applied models are two-equation models, except for the Spalart – Allmaras model, which is a one-equation model. The need for using turbulence models arises at higher Reynolds numbers (around $Re = 10^5$ for external flows). Turbulence models have the ability to predict and simulate complex turbulent flows, enabling adequate further optimization in future simulations.

The 3D numerical flow computation is based on a density-based solver [17] with a k – w SST [18] turbulence model. It solves the main equations of continuity, momentum, and energy simultaneously. Two algorithms are available for solving these sets of equations: implicit and explicit. For the purpose of the

calculation presented in the paper, the implicit method was implemented. It should be clearly mentioned that the employed 3D model assumes an infinite wing (which is achieved by defining periodic boundary conditions on the sides). Therefore, the obtained aerodynamic coefficients correspond to a wing of infinite aspect ratio (airfoil), and tip losses and induced drag are not accounted for in any way (since there are no wing tips).

The k – w SST model has proven to be an exceptionally effective method for examining turbulent flows in aerospace engineering applications. This approach combines the advantages of both the k - ε and k – w [19] models, making it a powerful tool for simulating turbulent flow dynamics.

3.1 Computational Domain and Meshes

The geometry of the airfoil was imported into Design Modeler, where the geometric characteristics of the computational domain were further defined. The domain is of type C, with 20 chord lengths in front of and on the sides and 30 chord lengths behind the airfoil. In the case of the 3D domain, it consists of an extruded domain for one chord length of the 2D geometry, which is deemed sufficient to encompass the 3D flow and allows for the development of spatial turbulent flow structures.

Hexa Mesh - The 2D domain (Figure 2) was discretized using Hexa-type mesh elements, which are categorized as simple mesh types and offer a fast and relatively reliable solution. They are primarily utilized in preliminary 2D computations. During the mesh generation process, all quality criteria were adhered to, resulting in an approximate total of 200,000 elements.

The specified number of mesh cells is considered satisfactory, as confirmed by the study presented in reference [13].

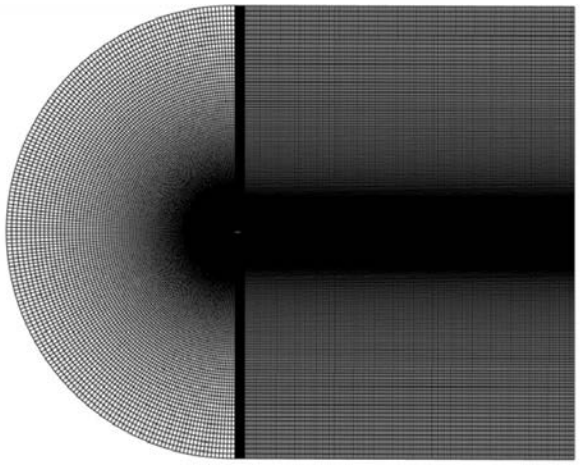

Figure 2. Computational C - Domain with Hexa-type elements of mesh

Poly Mesh - In this study, a domain was created and discretized using elements of mosaic technology for 3D flow analysis (Figure 3).

The poly mesh method is a relatively new approach to meshing that has shown very satisfying results in terms of accuracy and efficiency. However, further testing is still required to confirm its effectiveness. This study aims to address that need by evaluating the poly mesh method, in contrast to more conventional approaches.

This type of mesh exhibits a high level of adaptability to complex geometries, making it highly efficient for solving intricate numerical computations. The computational time is shorter compared to standard meshes, which contributes to its rising popularity among engineers. Due to the “mosaic” geometry, it uses a smaller number of elements or nodes, allowing for fine mesh refinement in critical areas of the model, while coarser elements can be used in other parts of the domain. This approach doesn’t affect the accuracy of the results but significantly reduces computation time [20] [21].

The results obtained using this mesh are presented in the subsequent sections of the paper, with the total number of mesh cells approximating 300,000. The calculations were performed using a simpler and more complex coarse and fine mesh, which requires a longer computational time. However, the results obtained from both meshes were found to be consistent and identical to those obtained from this final mesh.

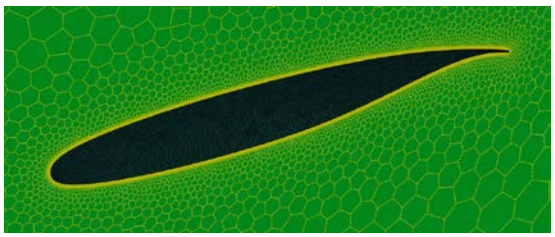

Figure 3. Poly Mesh with Mosaic elements

3.2 Numerical analysis - Solver

The methods and meshes employed in the numerical calculations must be validated against analytical or experimental data to ensure adequate accuracy with certainty. Ideally, experimental data are compared with numerical results, as analytical approaches have their limitations, especially in the transonic regime. Frequently, data may not be available for all cases, necessitating adjustments to the numerical computations based on existing data to define approaches and methods for various scenarios. The analyses are conducted at the same Mach and Reynolds numbers as those in the experimental investigations, specifically M = 0.5 and MRe = 4.4. The Reynolds number is regulated by the length of the chord, with fixed values of kinematic viscosity and Mach number.

The flow is steady, compressible (air is considered an ideal gas), and viscous with second-order discre–tization schemes. As previously stated, this applies to both cases, 2D and 3D.

For the 2D flow case, the boundary conditions are defined as follows: inlet-pressure far field and outlet-pressure outlet.

Pressure far-field is used for modeling flow around objects such as aircraft and other flying and nonflying objects such as cars. This type of boundary condition allows for achieving an effect where the object's influence on the flow is minimal. When setting this condition, temperature, static pressure, Mach number,

and flow direction relative to the object are defined, enabling precise analysis of aerodynamic phenomena.

The boundary conditions for the 3D flow are set as inlet-pressure far field, outlet-pressure outlet, and side surfaces – periodic. During both types of analyses, the temperature and pressure values applicable at sea level were considered, specifically T = 288.15 K and p = 101,325 Pa. The goal of the analyses is to determine Cn and Cd as functions of the angle of attack, which is defined based on the available experimental data. The geometry of the supersonic airfoil NASA SC (2) 0712 is illustrated in Figure 4.

Figure 4. The geometry of NASA sc (2) 0712 supercritical airfoil

4. RESULTS AND DISCUSSION

Experimental data are available for the modified NASA series (3) 0712. The difference between series 2 and 3 is illustrated in Figure 5. Data for airfoils of the same series and purpose, featuring a maximum relative thickness of 14%, are also accessible.

Although series 2 and 3 differ in the front part – lowest line of the airfoil, this difference significantly affects the drag coefficient. Any deviation from the original shape of the airfoil, particularly in the fore part of the airfoil contour, can impact the overall aerody–namic drag. Understanding these differences is crucial for optimizing aerodynamic performance.

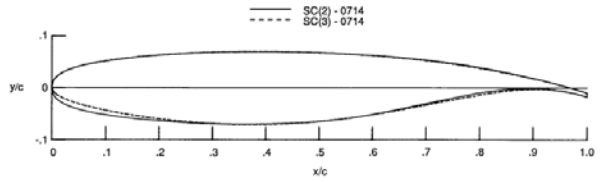

Figure 5. Geometric representation of the comparison between series 2 and 3

3.3 Aerodynamic Coefficients

The results obtained from the CFD calculations were further compared with the results from the Panel Method implemented in the Java Foil program, which is accessible online through the BigFoil [22].

It is acknowledged that Java Foil also has its limitations, which arise from the assumption of potential flow. As mentioned previously, this means that the direct effect of viscosity is not considered but is instead taken into account indirectly through corrections. While this method is efficient for preliminary and quick 2D analysis, it is not accurate enough for flow regimes where turbulence and viscosity are key factors – such as in the boundary layer, at higher angles of attack, and at higher speeds.

In the case of this airfoil, considering all available data, the Java Foil method did not provide satisfactory correlations.

The normal force coefficient Cn, calculated nume–rically using the CFD method and illustrated in Figure 6, aligns satisfactorily with the experimental data in both the 2D and 3D flow scenarios.

It is immediately apparent that the potential flow model yields a significantly higher normal force gra–dient, while all turbulence models produce similar results for both 2D and even 3D geometries (Figure 6).

The results obtained from the CFD simulation and their deviations from the experimental data are presented in Tables (1 – 6).

The results obtained from the numerical CFD simulation and their deviations from the experimental data are presented in Tables (1 – 6). Apparently, large values of relative errors at the angle-of-attack of −4° may be attributed to the near-zero values of normal force coefficient and consequential division by the near-zero denominator. Otherwise, the relative differences are acceptable for both investigated aerodynamic coef–ficients. The normal coefficient seems to be more accurately estimated at higher angles-of-attack, whereas the drag coefficient appears the most accurate at zero angle-of-attack. It should be borne in mind that some experimental errors are also present (but unfortunately, cannot be accurately estimated). Additionally, the nose part of the airfoil contours used in the experimental and computational campaigns, respectively, differs slightly, which mainly affects the drag coefficient.

Table 1. Experimental Data from Nasa Report [10]

α [˚]	Cn	Cd
–4	–0.0386	0.0102
0	0.4125	0.0097
2	0.6193	0.0104
3.4	0.7963	0.0114

Table 2. 2D case – results and absolute error between numerical and experimental case – k ε standard numerical model

α [˚]	Cn	Cd	Δx_Cn[%]	Δx_Cd[%]
–4	–0.0708	0.0172	**83.39**	**68.29**
0	0.4645	0.0118	**12.62**	**22.35**
2	0.6784	0.0148	**9.53**	**43.07**
3.4	0.8169	0.0181	**2.58**	**59.18**

Table 3. 2D case – results and absolute error between nume–rical and experimental case – k ε realizable numerical model

α [˚]	Cn	Cd	Δx_Cn[%]	Δx_Cd[%]
–4	–0.0583	0.0147	**50.95**	**43.99**
0	0.4653	0.0116	**12.8**	**19.86**
2	0.6814	0.0145	**10.01**	**39.66**
3.4	0.8217	0.0176	**3.19**	**54.25**

Table 4. 2D case – results and absolute error between numerical and experimental case – Spalart-Allmaras numerical model

α [˚]	Cn	Cd	Δx_Cn[%]	Δx_Cd[%]
–4	–0.0751	0.0155	**94.29**	**51.49**
0	0.4645	0.0111	**11.88**	**15.22**
2	0.6718	0.0134	**8.47**	**34.83**
3.4	0.7999	0.0171	**0.45**	**49.83**

Table 5. 2D case – results and absolute error between numerical and experimental case – k ω SST numerical model

α [˚]	Cn	Cd	Δx_Cn[%]	Δx_Cd[%]
–4	–0.0579	0.0156	**50.01**	**52.75**

0	0.4577	0.0115	**10.97**	**19.01**
2	0.6759	0.0144	**9.13**	**38.86**
3.4	0.8162	0.0174	**2.50**	**52.72**

Table 6. 3D case – results and absolute error between numerical and experimental case – Poly Mesh

α [˚]	Cn	Cd	Δx_Cn[%]	Δx_Cd[%]
–4	0.0206	0.0089	**153.37**	**12.75**
0	0.4565	0.0099	**10.67**	**3.14**
2	0.6687	0.0119	**7.97**	**14.61**
3.4	0.8071	0.0139	**1.35**	**22.47**

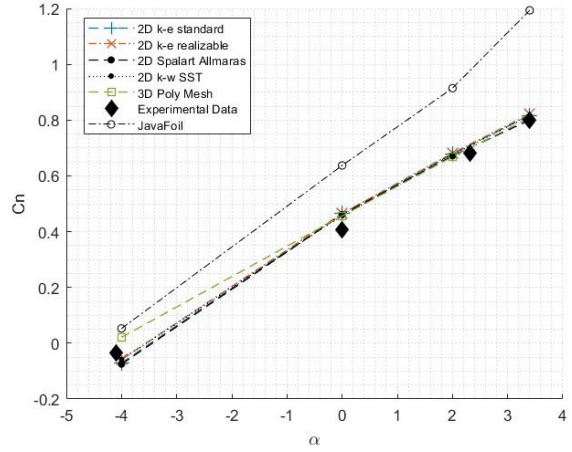

Figure 6. Coefficient of normal force as a function of AOA

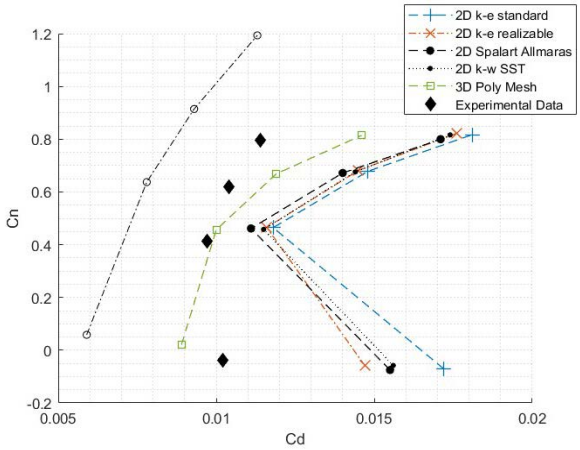

Figure 7. Drag coefficient as a function of Cn

In the 3D simulation results (Table 6), significant discrepancies are observed in the prediction of coef–ficients at negative angles of attack and near zero angles of attack. This phenomenon arises due to the nonlinear behavior of aerodynamic forces, making it impossible to accurately model the flow in this regime using simple standard approximations.

The turbulent models presented in Figure 6 show adequate agreement with the experimental data (both cases – 2D and 3D). No significant deviations were observed, indicating that the estimation of Cn through numerical calculations is highly satisfactory. The best matches are observed at zero angle of attack, as well as at the optimal angle of attack.

When estimating drag as a function of the normal force coefficient, larger deviations occur in the 2D case. Accordingly, a polyhedral mesh was introduced for estimating drag in 3D flow, and the results are presented in Figure 7.

3.4 Flow visualization

After completing the numerical calculations, one method for verifying the results involves analyzing the contours around the airfoil. In this context, particular attention is given to the turbulence occurring behind the airfoil, as well as the contours of the Mach number and Static Pressure.

Visualization of turbulence in the previous analyses is crucial for understanding the differences in drag that occur between 2D and 3D analyses (Figure 8.a and Figure 8.b).

3D flow represents a more challenging approach in numerical analysis, as it considers all effects that occur during 3D flow, which are neglected in 2D flow. On the other hand, 2D calculations are simpler and provide a quick insight into the results.

The results of this study indicate a significant diffe–rence between 2D and 3D analyses, with the 3D com–putation showing better agreement with existing expe–rimental data. The similarity between the turbulent mo–dels applied in the 2D analysis is high, which is why one of the tested 2D models was used for the 3D case (k – ω SST). While the 2D case was analyzed using a pressure-based solver, the 3D case was solved with a density-based solver. Additionally, there is a difference in the type of mesh used in both cases. Considering all the factors that may influence the results, the 3D analysis provided much better agreement compared to the 2D analysis.

The effects of 2D flow are illustrated in Figure 8.a, where it can be observed that the flow is exclusively planar and smooth, almost without any turbulence except in the narrow region directly originating from the blunt trailing edge. In contrast, Figure 8.b shows that the flow in the domain of the airfoil is uniform, while turbulence can be observed behind the airfoil, which has been accounted for in the overall drag. Thickening of the boundary layer can also be observed, etc.

The visualization represented in this paper was conducted for a M = 0.5, 4.4 MRe, and AOA = 0° [10].

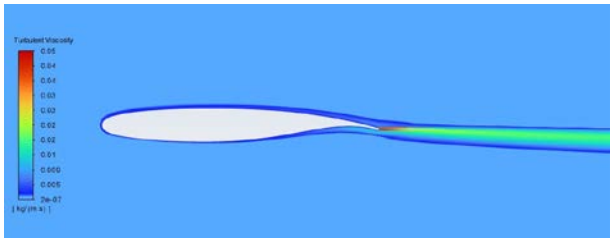

Figure 8.a Turbulent Viscosity around NASA sc (2) 0712 at AOA 0° – 2D case

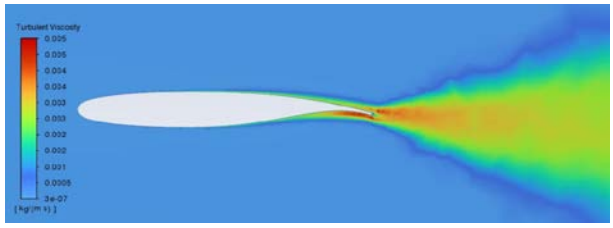

Figure 8.b Turbulent Viscosity around NASA sc (2) 0712 at AOA 0° – 3D case

The visualization shown in Figure 9 represents a 3D flow case, with the flow observed from a different perspective. The visualization method used is crucial for

assessing flow behavior, as it provides a detailed insight into turbulent phenomena. It can be observed that the flow is attached to both the upper and lower surfaces of the airfoil, without separation, exhibiting mild turbu–lence behind the trailing edge which matches the visu–alization from Figure 8.b.

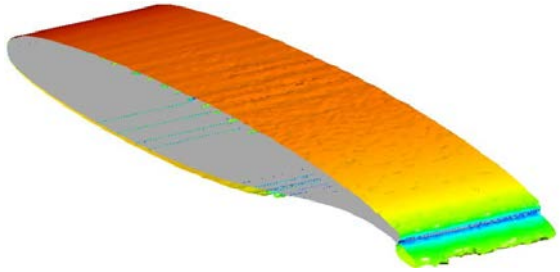

Figure 9. Turbulent Viscosity around NASA sc (2) 0712 at AOA 0° - 3D case

Visualization of Mach number contours is essential for interpreting results during verification. The Figures 10 and 11 reveal characteristics of supercritical airfoils, where the Mach number on the upper surface is higher than on the lower surface due to the nature of geometry – curvature of the airfoil. Additionally, it can be observed that the trailing shock wave is avoided (M = 0.5).

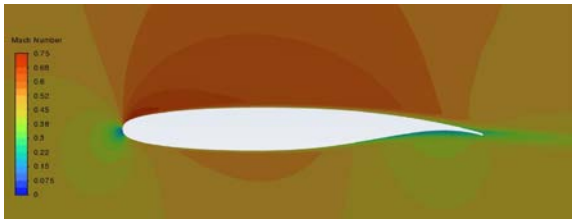

Figure 10. Mach number contour around NASA sc (2) 0712 at AOA 0° - 2D case

Figure 11. Mach number contour around NASA sc (2) 0712 at AOA 0° – 3D case

3.5 Pressure distribution

The representation of the pressure coefficient reveals a stagnation point that moves along the airfoil nose depending on the specified flow conditions. Additi–onally, the zones of low pressure on the upper surface of the airfoil and the zones of high pressure on the lower surface are clearly represented in Figures 12 and 13.

The flow is attached without separation, which is expected for the NASA sc(2) 0712 airfoil, which is designed to minimize wave drag at high speeds.

Figures 14, 15, and 16 show the effect of changing the angle of attack of the airfoil, specifically illustrating how the pressure coefficient distribution along the chord varies.

At Figure 15, it can be observed that the flow is uniform, characterized by the absence of abrupt changes in the pressure coefficient along the chord.

During the analysis of the Cp at AOA of –4° (Figure 16), a decrease in pressure on the upper surface of the airfoil is observed, along with an increase on the lower surface. This change results in a reduction in lift and an increase in drag of the airfoil.

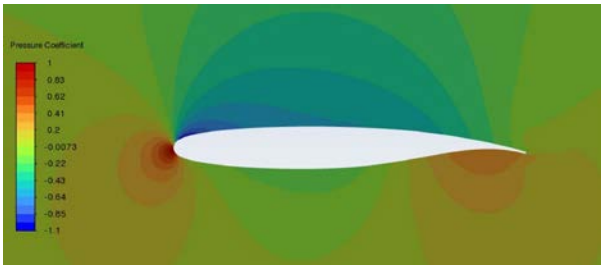

Figure 12. Pressure coefficient - NASAsc(2) 0712 at AOA 0° - 2D case

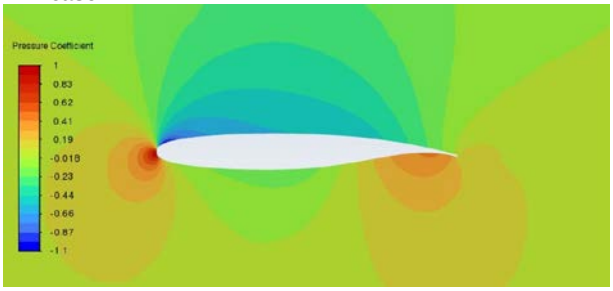

Figure 13. Pressure coefficient – NASA sc (2) 0712 at AOA 0° - 3D case

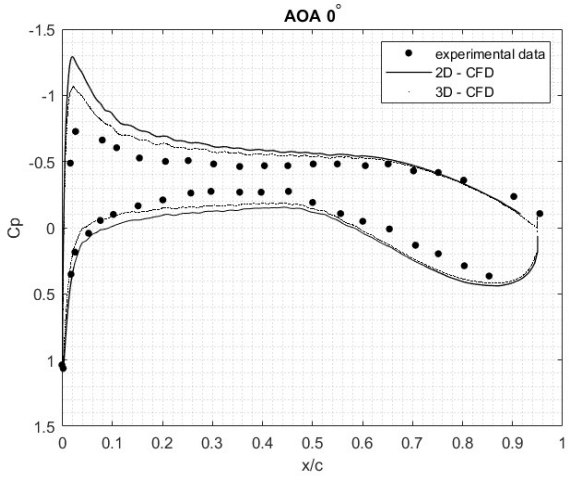

Figure 14. Cp – NASA sc (2) 0712 at AOA 0°

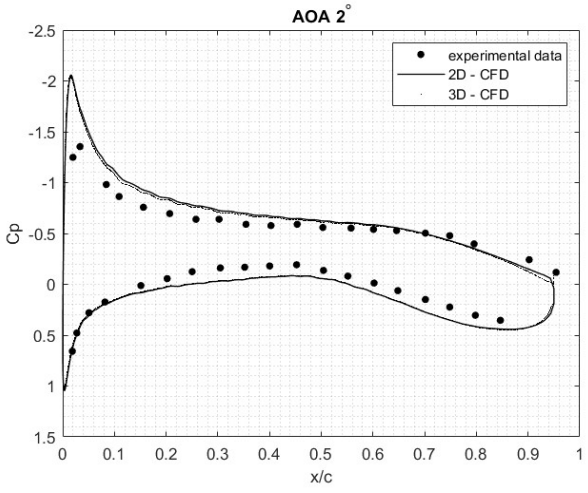

Figure 15. Cp – NASA sc (2) 0712 at AOA 2°

The discrepancies between the experimental and numerical values of the pressure coefficient are greater in the fore part of the lower (pressure) side of the airfoil, which is primarily caused by the slight geometric differences. Otherwise, the trends of the chordwise pressure distributions with the changing angle-of-attack are completely captured, particularly with the 3D set-up at a lower angle-of-attack. Again, experimental values also contain certain measurement errors, that cannot be quantified in more detail.

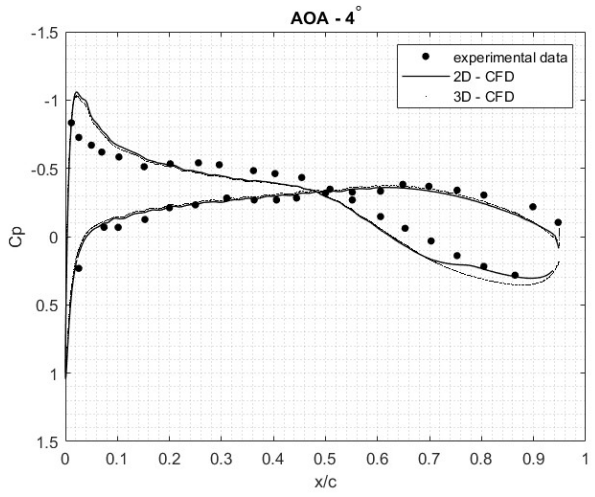

Figure 16. Cp – NASA sc (2) 0712 at AOA – 4°

5. CONCLUSION

In this paper, two approaches to airfoil analysis were applied in parallel to achieve an optimal analysis that will be implemented in future calculations. Initially, 2D flow was examined using hexa type of mesh elements, employing four different turbulence models.

Subsequently, the same airfoil was analyzed in three dimensions by introducing 3D calculations and utilizing the well-known k – w SST numerical model with mo–saic poly mesh elements. Both approaches were com–pared with experimental data as well as with the panel method and their agreement was interpreted and pre–sented.

A discrepancy in the results of the numerical calculation of the drag coefficient Cd was observed in the 2D flow case. However, by implementing the 3D flow domain, excellent correlations between the experi–mental data and the numerical calculations were achi–eved. The deviation from the experimental values in the 3D numerical simulation has been reduced by appro–ximately 30% (20% at smaller AOA) compared to the values obtained during the 2D simulation.

2D analyses often yield higher values of the drag coefficient compared to 3D flow. These overestimated measurements result from simplified assumptions about flow and interactions with the surrounding fluid, which can lead to inaccurate assessments of aerodynamic per–formance. In this sense, 2D analyses can be used only for preliminary studies, with a certain degree of caution.

In contrast, 3D simulations account for the comp–lexity of flow (particularly in the fore/nose and aft/ trailing zones of the airfoil), allowing for a better un–derstanding of actual flight conditions and a more precise determination of the drag coefficient. The relative error in the drag coefficients remains below 10%. These findings highlight the importance of using advanced models for accurate analysis and optimization of airfoils.

In the Master Thesis [9], a detailed analysis of this airfoil was conducted at various Reynolds and Mach numbers. Through the set of analyses of the 2D cases presented in the paper, it was determined that the 2D model overestimates drag. Consequently, this implies a twofold confirmation of the 2D case suboptimality in terms of more detailed flow investigations.

With this level of reliability, we can confidently perform calculations for other cases of flow as well.

REFERENCES

[1] J. Arramach, N. Boutammachte, A.Bouatem, A. Al Mers: *A Novel Technique for the Calculation of Pos t–Stall Aerodynamic Coefficient for S809 Airfoil,* FME Transactions, Vol. 48, No.1, pp: 117 – 126, 2020.

[2] Yuwei Cheng, Jinyuan Zeng, Qian Chen, Haizhao Liang, Peng Bai: *Aerodynamic Characteristic of Morphing Supercritical Airfoils for Aircraft with All–Stage High Performance,* Appl. Sci. 2022, 12, 1128.

[3] Dawei Liu, Yuanjing Wang, Dehua Chen, Xin Peng, Xing Xu: *Numerical Investigation on the Reynolds Number Effect of Supercritical Airfoil,* Procedia Engineering, Volume 31, pp: 109 – 109, 2012.

[4] T V Poplavskaya et al.: *Numerical simulation of the transition to turbulence in subsonic and transonic flow,* J. Phys.: Conf. Ser. 1359 012068, 2019.

[5] Ivan.A. Kostić, Zorana A. Stefanović, Olivera P. Kostić*: Aerodynamic Analysis of a Light Aircraft at Different Design Stages*, FME Transactions, Vol. 42, No. 2, pp: 94 – 105, 2014.

[6] Goran Ocokoljić, Dijana Damljanović, Đorđe Vuković, Boško Rašuo: *Contemporary Frame of Measurement and Assessment of Wind – Tunnel Flow Quality in a Low–Speed Facility*, FME Transactions, Vol.46, No. 4, pp: 429 – 442, 2018.

[7] Bosko Rasuo: *Scaling between Wind Tunnels – Results Accuracy in Two-Dimensional Testing*, Transactions of the Japan Society for Aeronautical and Space Sciences, Vol.55, No. 2, pp: 109-115, 2012.

[8] Bosko Rasuo: *The Influence of Reynolds and Mach numbers on two-dimensional wind-tunnel testing: An experience*, The Aeronautical Journal, Vol. 115, No. 1166, pp: 249 – 254, April 2011.

[9] C.D Harris: *NASA Supercritical Airfoils – A Matrix of Family – Related Airfoils*, National Aeronautics and Space Administration – NASA, Technical Paper 2969, Langley Research Center, Hampton, Virginia, 1990.

[10] W.G. Johnson, Jr., Acquilla S. Hill, and Otto Eichmann: *High Reynolds Number Tests of a NASA SC (3) – 0712(B) Airfoil in the Langley 0.3-Meter Transonic Cryogenic Tunnel*, National Aeronautics and Space Administration - NASA, Technical Memorandum 86371, June 1985.

[11] Xuyang Bai: *Study and analysis of lift to drag ratio performance of supercritical wing based on computational fluid dynamics method*, J. Phys.: Conf. Ser. 2634 012018, 2023.

[12] Jovan Lj Miljanić: *Numerička analiza okozvučnog opstrujavanja superkritičnog aeroprofila NASA sc(3)-0712(B) (in Serbian)*, Master Thesis, University of Belgrade, Faculty of Mechanical Engineering, Belgrade, 2024.

[13] Wiliam E. Milholen II, Lewis R. Owens: *On the Application of Contour Bumps for Transonic Drag Reduction (Invited)*, NASA Langley Research Center, Hampton, VA, 23681 – 2199, AIAA – 2005-0462.

[14] R. Johnson. At last: *An instrument that reads drag!* Soaring, 47(10), October 1983.

[15] Yorick Abraham de Valk: *A Novel Construction of Wind Tunnel models for wind energy applications*, MSc Thesis, University of Twente Department of Engineering Technology, EFD – 331, 20. 12. 2019.

[16] ANSYS FLUENT: Introduction to Ansys Fluent, *Lecture 6, Turbulence Modeling*, Fluent Inc., Centerra Recourse Park, 10 Cavendish Court, Lebanon, NH 03766, 2010.

[17] ANSYS FLUENT: *Fluent 6.3, Tutorial Guide*, Ansys Fluent Documentation, September 2006.

[18] ANSYS FLUENT 12.0: *Theory Guide, 4.5.2 Shear-Stress Transport (SST) k - w Model*, Ansys, Inc. 23.01.2009.

[19] Inamul Hasan, R. Mukesh, P. Radha Krishnan, R. Srinath, R.B. Dhanya Prakash: *Forward Flight Performance Analysis of Supercritical Airfoil in Helicopter Main Rotor*, Intelligent Automation & Soft Computing, Vol.33, No.1, 2022.

[20] ANSYS Fluent Mosaic Technology: *Ansys Fluent Mosaic Technology Automatically Combines Disparate Meshes with Polyhedral Elements for Fast, Accurate Flow Resolution*, Ansys Fluent Documentation, Canonsburg, PA, 2020.

[21] Amjd Ibraheem: *Evaluating the Efficiency of Polyhedral Mesh Elements in Solving the Problem of the Flow around Ship's Rudder*, International Journal of Engineering and Management Sciences (IJEMS), Vol. 6, No. 2, pp. 241 – 256, 2021.

[22] Big Foil, „SC (2) 0712", Accessed 12.09.2024 https://www.bigfoil.com/7c63ec05-0593-4d43-a75e-60ccbb55ab22_info.php

NOMENCLATURE

α	Angle of attack of airfoil [˚]
Cn	Normal force coefficient
Cd	Drag force coefficient
Cp	Pressure coefficient
M	Mach number
MRe	Mega Reynolds number / Rex10^6
CFD	Computational Fluid Dynamics
NASA	National Aeronautical and Space Administration
ATAT	Advances Technology Airfoil Test
AOA	Angle of Attack
RANS	Reynolds – Averaged Navier Stokes
SST	Shear Stress Transport

ПРОЦЕНА АЕРОДИНАМИЧКИХ КОЕФИЦИЈЕНАТА СУПЕРКРИТИЧНОГ АЕРОПРОФИЛА НАСА СЦ(2) 0712: УПОРЕДНА СТУДИЈА 2Д И 3Д МОДЕЛА ТОКА СА ЕКСПЕРИМЕНТАЛНИМ ВАЛИДАЦИЈАМА

Т. Шукунда, Ј. Сворцан, Т. Иванов

Ова студија представља компаративну нумеричку анализу 2Д и 3Д компресибилних, турбулентних струјања око суперкритичног аеропрофила НАСА сц(2) 0712 при Маховом броју M = 0,5 користећи метод коначних запремина имплементиран у АНСИС Флуент, фокусирајући се на процену коефицијената отпора у односу на постојеће експерименталне податке. Поред тога, тестирају се различите врсте рачунарских мрежа и модела турбуленције. Истраживање има за циљ да истакне уочене разлике између два приступа моделирању и њихове импликације на предвиђања аеродинамичких перформанси. Кроз ригорозне нумеричке симулације и валидацију у односу на експерименталне резултате, показали смо да 2Д модели често дају прецењене вредности отпора због поједностављених претпоставки протока. Насупрот томе, 3Д симулације пружају прецизнији приказ понашања флуида, што резултира ближим усклађивањем са експерименталним налазима. Извођењем просторних прорачуна турбулентног струјања око суперкритичног аеропрофила, могуће је смањити релативну грешку коефицијената отпора за мање од 10%.